Available online at www.CivileJournal.org

Civil Engineering Journal

Vol. 6, No. 3, March, 2020

R-function Theory for Bending Problem of Shallow Spherical Shells with Polygonal Boundary

Shanqing Li [a], Hong Yuan [a*], Xiongfei Yang [a], Huanliang Zhang [a], Qifeng Peng [a]

[a] *MOE Key Laboratory of Disaster Forecast and Control in Engineering, School of Mechanics and Construction Engineering, Institute of Applied Mechanics, Jinan University, Guangzhou 510632, China.*

Received 31 October 2019; Accepted 07 January 2020

Abstract

The governing differential equations of the bending problem of simply supported shallow spherical shells on Winkler foundation are simplified to an independent equation of radial deflection. The independent equation of radial deflection is decomposed to two Laplace operators by intermediate variable. The R-function theory is applied to describe a shallow spherical shell on Winkler foundation with concave boundary, and then a quasi-Green's function is established by using the fundamental solution and the normalized boundary equation. The quasi-Green's function satisfies the homogeneous boundary condition of the problem. The Laplace operators of the problem are reduced to two simultaneous Fredholm integral equations of the second kind by the Green's formula. The singularity of the kernel of the integral equation is eliminated by choosing a suitable form of the normalized boundary equation. The integral equations are discretized into the homogeneous linear algebraic equations to proceed numerical computing. The singular term in the discrete equation is eliminated by the integral method. Some numerical examples are given to verify the validity of the proposed method in calculating simple boundary conditions and polygonal boundary conditions. A comparison with the ANSYS finite element (FEM) solution shows a good agreement, and it demonstrates the feasibility and efficiency of the present method.

Keywords: Green's Function; R-function; Integral Equation; Bending of Shallow Spherical Shell; Concave Boundary.

1. Introduction

As a kind of structural forms, the shells and plates are widely used in various fields, such as, in the large-span roof, the underground foundation engineering, the hydraulic engineering, the large container manufacturing, the aviation, the shipbuilding, the missiles, the space technology, the chemical industry, and so on. Only few problems of the shells and plates with a regular geometric boundary and a simple differential equation can be solved with an analytical or a half analytical method. For most these problems with geometry of arbitrary shape and a complex boundary condition, only numerical methods can be used to solve the problems, such as the boundary element method [1], the Finite Element Method [2] and the finite difference method [3].

In the present paper, the R-function theory and the quasi-Green's function method (QGFM) proposed by Rvachev [4] are utilized. The bending problem of simply supported dodecagon shallow spherical shells on Winkler foundation with concave boundary is studied. The governing differential equation of the problem is decomposed into two simultaneous differential equations of lower order by utilizing an intermediate variable. A quasi-Green's function is established by using the fundamental solution and the boundary equation of the problem. This function satisfies the

* Corresponding author: tyuanhong@jnu.edu.cn

http://dx.doi.org/10.28991/cej-2020-03091487

homogeneous boundary condition of the problem, but it does not satisfy the fundamental differential equation. The key point of establishing the quasi-Green's function consists in describing the boundary of the problem by a normalized equation $\omega = 0$ and the domain of the problem by an inequality $\omega > 0$. There are multiple choices for the normalized boundary equation. Based on a suitably chosen normalized boundary equation, a new normalized boundary equation can be established such that the singularity of the kernel of the integral equation is overcome. For any complicated domain, a normalized boundary equation can always be found according to the R-function theory. Thus, the problem can always be reduced to two simultaneous Fredholm integral equations of the second kind without the singularity. Using the R-function theory, Li and Yuan described successfully the rectangular, trapezoidal, triangular and parallelogrammic domains of plates [5-7] and shallow spherical shells [8, 9]. For the first time, the R-function theory is applied to describe the dodecagon domain of the shallow spherical shells with concave boundary. The flowchart of research methodology is shown in the paper. The governing differential equations of the bending problem of simply supported shallow spherical shells on Winkler foundation are simplified to an independent equation of radial deflection. The intermediate variable is introduced, and then the independent equation of radial deflection is decomposed to two Laplace operators. The Laplace operators of the problem are reduced to two simultaneous Fredholm integral equations of the second kind by the Green's formula. The singularity of the kernel of the integral equation is eliminated by choosing a suitable form of the normalized boundary equation. The integral equations are discretized into the homogeneous linear algebraic equations to proceed numerical computing. The singular term in the discrete equation is eliminated by the integral method. Some numerical examples are given to verify the validity of the proposed method in calculating simple boundary conditions and polygonal boundary conditions. A comparison with the FEM solution shows a good agreement, and it demonstrates the feasibility and efficiency of the present method. The R-function theory can be used to describe any more complex domains of the plates and shells.

2. Research Methodology

Flowchart of the research methodology has been presented in Figure 1.

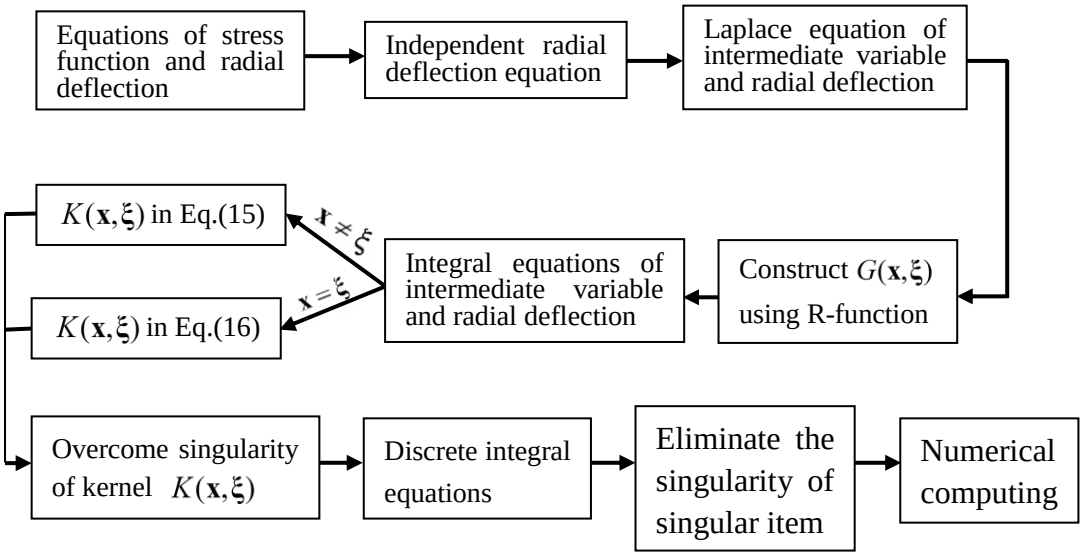

Figure 1. The flowchart of research methodology

2.1. Fundamental Equations

The governing differential equations of the bending problem of simply supported shallow spherical shells on Winkler foundation [9, 11-16] can be expressed as follows:

$$\nabla^4 \varphi(\mathbf{x}) - \frac{Eh}{R}\nabla^2 w(\mathbf{x}) = 0, \quad \mathbf{x} \in \Omega \tag{1}$$

$$D\nabla^4 w(\mathbf{x}) + \frac{1}{R}\nabla^2 \varphi(\mathbf{x}) + kw(\mathbf{x}) = P_Z, \quad \mathbf{x} \in \Omega \tag{2}$$

Where $\nabla^4 = (\partial^2/\partial x_1^2 + \partial^2/\partial x_2^2)^2$ is the biharmonic operator, φ is the stress function, w is the radial deflection of the shell, R is the radius of curvature of the shell, k is the elastic coefficient of the foundation, $\mathbf{x} = (x_1, x_2)$, Ω is the domain of the trapezoid of shallow spherical shells in Cartesian coordinates, P_Z is the radial load; and $D = Eh^3/(12(1-\nu^2))$ is the flexural rigidity of the shell, in which h is the thickness of the shell, and E and ν are Young's modulus and Poisson's ratio, respectively.

The simply supported boundary conditions can be written as:

$$w\big|_{\Gamma} = \nabla^2 w\big|_{\Gamma} = \varphi\big|_{\Gamma} = \nabla^2 \varphi\big|_{\Gamma} = 0 \tag{3}$$

Where $\nabla^2 = \partial^2/\partial x_1^2 + \partial^2/\partial x_2^2$ is the Laplace operator, and $\Gamma = \partial\Omega$ is the boundary of the domain Ω.Making use of Equations 1 and 3, we can easily obtain:

$$\nabla^2 \varphi = wEh/R \tag{4}$$

Substituting Equation 4 into Equation 2 yields:

$$D\nabla^4 w + wEh/R^2 + kw = P_Z \tag{5}$$

To decompose Equation 5, let us introduce the following intermediate variable;

$$M = (M_1 + M_2)/(1+\nu) \tag{6}$$

Where $M_1 = -D(\partial^2 w/\partial x_1^2 + \nu\partial^2 w/\partial x_2^2)$ and $M_2 = -D(\partial^2 w/\partial x_2^2 + \nu\partial^2 w/\partial x_1^2)$.

Then, substituting Equation 6 into Equation 5, we obtain the following two simultaneous Laplace equations [17-20] of second rank:

$$\nabla^2 M = -P_Z + wEh/R^2 + kw \text{ and } \nabla^2 w = -M/D, \quad \mathbf{x} \in \Omega \tag{7}$$

The displacement and the bending moment should be equal to zero along the simply supported boundary of shallow spherical shells on Winkler foundation, which can be written as:

$$w = 0 \text{ and } M = 0, \quad \mathbf{x} \in \Gamma \tag{8}$$

2.2. Integral Equations

The complicated domain can be describing by Boolean operation. The Boolean operations $\vee_\alpha$, $\wedge_\alpha$ (disjunction and conjunction), which correspond to the union ∪ and intersection ∩. These R-operations are defined as follows [1]:

$$X \wedge_\alpha Y = \frac{1}{1+\alpha}(X + Y + \sqrt{X^2 + Y^2 - 2\alpha XY}), \; X \vee_\alpha Y = \frac{1}{1+\alpha}(X + Y - \sqrt{X^2 + Y^2 - 2\alpha XY})$$

Where the parameter α varies within $-1 < \alpha \leq$. For example, if the value α is equal to zero, then the whole domain can be presented using R-function.

Let $\omega = 0$ be the normalized boundary equation of the first-order on the boundary Γ, i.e. [4]:

$$\omega(\mathbf{x}) = 0, \; |\nabla\omega| = 1, \quad \mathbf{x} \in \Gamma \text{ and } \omega(\mathbf{x}) > 0, \quad \mathbf{x} \in \Omega \tag{9}$$

The quasi-Green's function can be established as follows:

$$G(\mathbf{x},\boldsymbol{\xi}) = \frac{1}{2\pi}\ln r - \frac{1}{2\pi}\ln R_1 \tag{10}$$

Where $r = \|\boldsymbol{\xi} - \mathbf{x}\| = \sqrt{(\xi_1 - x_1)^2 + (\xi_2 - x_2)^2}$ and $R_1 = \sqrt{r^2 + 4\omega(\boldsymbol{\xi})\omega(\mathbf{x})}$, in which $\mathbf{x} = (x_1, x_2)$ and $\boldsymbol{\xi} = (\xi_1, \xi_2)$. Obviously, the quasi-Green's function $G(\mathbf{x},\boldsymbol{\xi})$ satisfies the following condition:

$$G(\mathbf{x},\boldsymbol{\xi})\big|_{\boldsymbol{\xi}\in\partial\Omega} = 0 \tag{11}$$

To reduce the boundary value problems Equations 7 and 8 into the integral equations, the following Green's formula of sets of function $C^2(\Omega)$, i.e., U and $V \in C^2(\Omega \cup \Gamma)$, is applied:

$$\int_{\Omega}(V\nabla^2 U - U\nabla^2 V)\,\mathrm{d}_{\xi}\Omega = \int_{\Gamma}(V\frac{\partial U}{\partial n} - U\frac{\partial V}{\partial n})\,\mathrm{d}_{\xi}\Gamma \tag{12}$$

From Equations 7, 8, 11 and 12, and noticing that $(1/2\pi)\ln r$ is the fundamental solution [21] of the Laplace operator, then the following integral equations are obtained:

$$w(\mathbf{x}) = -\frac{1}{D}\int_{\Omega} G(\mathbf{x},\boldsymbol{\xi})M(\boldsymbol{\xi})\,\mathrm{d}_{\xi}\Omega + \int_{\Omega} w(\boldsymbol{\xi})K(\mathbf{x},\boldsymbol{\xi})\,\mathrm{d}_{\xi}\Omega \tag{13}$$

$$M(\mathbf{x}) = \int_{\Omega} G(\mathbf{x},\boldsymbol{\xi})[-P_Z(\boldsymbol{\xi}) + \frac{Eh}{R^2}w(\boldsymbol{\xi}) + kw(\boldsymbol{\xi})]\,\mathrm{d}_{\xi}\Omega + \int_{\Omega} M(\boldsymbol{\xi})K(\mathbf{x},\boldsymbol{\xi})\,\mathrm{d}_{\xi}\Omega \tag{14}$$

Where;

$$K(\mathbf{x},\xi)=[R_1^{\,2}\omega(\mathbf{x})\nabla^2\omega+4\omega(\mathbf{x})\omega-4(\mathbf{r}\cdot\nabla\omega)\omega(\mathbf{x})-4\omega^2(\mathbf{x})(\nabla\omega)^2]/\pi R_1^{\,4} \tag{15}$$

Where $\omega=\omega(\xi)$, $\nabla=\nabla_\xi$; and $\mathbf{r}=(\xi_1-x_1)\mathbf{i}+(\xi_2-x_2)\mathbf{j}$, in which $\mathbf{i}$ and $\mathbf{j}$ denote unit vectors in x_1 and x_2 directions, respectively.

$K(\mathbf{x},\xi)$ in Equation 15 appears discontinuous only if $R=0$, i.e., both $\mathbf{x}=\xi$ and $\omega=0$ come into existence. Actually, when $\mathbf{x}=\xi$, Equation 15 can be reduced to:

$$K(\mathbf{x},\xi)\big|_{\mathbf{x}=\xi}=[1+\omega\nabla^2\omega-(\nabla\omega)^2]/4\pi\omega^2 \tag{16}$$

To make the kernel of the integral equations $K(\mathbf{x},\xi)\in C(\Omega\bigcup\partial\Omega)$, A normalized boundary equation will be constructed to ensure the continuity of $K(\mathbf{x},\xi)$ in the following. It can be easily testified that:

$$\omega=[3\omega_0+\omega_0^2\nabla^2\omega_0-\omega_0(\nabla\omega_0)^2]/2 \tag{17}$$

Where $\omega_0=0$ is the normalized equation on the boundary Γ, i.e., ω_0 satisfies Equation 9. Obviously, equation ω is also a normalized boundary equation of the first-order.

Based on a suitably chosen normalized boundary equation $\omega_0=0$, a new normalized boundary equation $\omega=0$ can be constructed by using Equation 17, which ensure the continuity of the integral kernel $K(\mathbf{x},\xi)$ in the integral domain.

2.3. Discrete Integral Equations

In order to discrete the integral Equations 13 and 14 of the bending problem of shallow spherical shell on Winkler foundation, the integral domain Ω is divide into several subdomains $\Omega_i(i=1,2,.....,N)$, and in each subdomain the rectangular quadrature formula is applied. Finally, integral Equations 13 and 14 are discretized into the following homogeneous linear algebraic equations:

$$\begin{bmatrix} A_{N\times N} & B_{N\times N} \\ C_{N\times N} & A_{N\times N} \end{bmatrix}[M(\mathbf{x}_1)\ \cdots\cdots\ M(\mathbf{x}_N)\ \ w(\mathbf{x}_1)\ \cdots\cdots\ w(\mathbf{x}_N)]^T=P_Z \tag{18}$$

Where $A_{N\times N}=(a_{ij})_{N\times N}$, when $i\neq j$, $a_{ij}=K(\mathbf{x}_i,\xi_j)A_j$; when $i=j$, $a_{ij}=K(\mathbf{x}_i,\xi_j)A_j-1$;

$B_{N\times N}=(b_{ij})_{N\times N}$, $b_{ij}=(\frac{Eh}{R^2}+k)G(\mathbf{x}_i,\xi_j)A_j$;

$C_{N\times N}=(c_{ij})_{N\times N}$, $c_{ij}=\frac{-G(\mathbf{x}_i,\xi_j)A_j}{D}$;

$P_Z=(p_k)_{2N\times1}$, when $k\leq N$, $p_k=p_i=Z\sum_{j=1}^{N}G(\mathbf{x}_i,\xi_j)A_j$, when $N<k\leq 2N$, $p_k=0$;

$(i=1,2,\cdots\cdots,N;\ j=1,2,\cdots\cdots,N;\ k=1,2,\cdots\cdots,2N)$;

In which A_i denotes the area of the i th subdomain.

When $\mathbf{x}_i=\xi_i$, r =0 of Equation 10, so the quasi-Green's function $G(\mathbf{x}_i,\xi_i)$ is singular item in Equation 10. In order to eliminate the singular term in the discrete Equation 18 of the integral equation, the integral formula of the subdomain is integrated, and the specific derivation process is as follows.

When $\mathbf{x}_i=\xi_i$, the integral formula of the Ω_i subdomain is integrated:

$$\int_{\Omega_i}G(\mathbf{x}_i,\xi)f(\xi)d_\xi\Omega_i=\frac{1}{2\pi}f(\xi_i)\int_{\Omega_i}\ln r\,d_\xi\Omega_i-q(\mathbf{x}_i,\xi_i)f(\xi_i)A_i \tag{19}$$

The first item of Equation 19 is singular item, in order to eliminate the singularity of this item, divide the subdomain into four small regions and integrate the item by parts (as Figure 2).

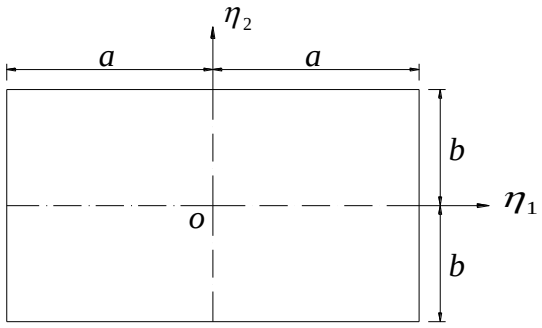

Figure 2. Rectangular subdomains

Set $\eta_1 = \xi_1 - x_1$, $\eta_2 = \xi_2 - x_2$, then the first term on the right of Equation 19 can be written as:

$$\frac{1}{2\pi} f(\xi_i)\int_{\Omega_i} \ln r d_{\xi}\Omega_i = \frac{1}{2\pi} f(\xi_i)\int_{-a}^{a}\int_{-b}^{b} \ln\sqrt{(\xi_1 - x_1)^2 + (\xi_2 - x_2)^2}\, d\eta_1 d\eta_2$$

$$= \frac{1}{2\pi} f(\xi_i)\left(\int_{-a}^{0}\int_{-b}^{0} \ln\sqrt{\eta_1^2 + \eta_2^2}\, d\eta_1 d\eta_2 + \int_{-a}^{0}\int_{0}^{b} \ln\sqrt{\eta_1^2 + \eta_2^2}\, d\eta_1 d\eta_2\right.$$

$$\left. + \int_{0}^{a}\int_{-b}^{0} \ln\sqrt{\eta_1^2 + \eta_2^2}\, d\eta_1 d\eta_2 + \int_{0}^{a}\int_{0}^{b} \ln\sqrt{\eta_1^2 + \eta_2^2}\, d\eta_1 d\eta_2\right)$$

$$= \frac{2}{\pi} f(\xi_i)\int_{0}^{a}\int_{0}^{b} \ln\sqrt{\eta_1^2 + \eta_2^2}\, d\eta_1 d\eta_2$$

$$= \frac{2}{\pi} f(\xi_i)\int_{0}^{a} d\eta_1 \left(\eta_2 \ln\sqrt{\eta_1^2 + \eta_2^2}\Big|_0^b - \int_0^b \eta_2 d\ln\sqrt{\eta_1^2 + \eta_2^2}\right)$$

$$= \frac{2}{\pi} f(\xi_i)\int_{0}^{a} d\eta_1 \left(b\ln\sqrt{\eta_1^2 + b^2} - \int_0^b \frac{\eta_2^2}{\eta_1^2 + \eta_2^2} d\eta_2\right) \tag{20}$$

In which,

$$\int_0^a b\cdot\ln\sqrt{\eta_1^2 + b^2}\, d\eta_1 = ab\ln\sqrt{a^2 + b^2} - ab + b^2 \arctan\frac{a}{b} \tag{21}$$

$$\int_0^a d\eta_1 \int_0^b \frac{\eta_2^2}{\eta_1^2 + \eta_2^2} d\eta_2 = \frac{ab}{2} - \frac{a^2}{2}\arctan\frac{b}{a} + \frac{b^2}{2}\arctan\frac{a}{b} \tag{22}$$

Substituting Equations 21 and 22 into Equation 20 gives:

$$\frac{1}{2\pi} f(\xi_i)\int_{\Omega_i} \ln r d_{\xi}\Omega_i = \frac{f(\xi_i)}{\pi}\left(2ab\ln\sqrt{a^2 + b^2} - 3ab + a^2\arctan\frac{b}{a} + b^2\arctan\frac{a}{b}\right) \tag{23}$$

Then, Equation 23 is the treatment of singular terms in the discretization equation. Subdomains of other shapes, such as triangle and trapezoid, can also be transformed into rectangular subdomains to eliminate singular terms in the discrete form of integral equation.

Then, the radial deflection $w(x_l)$ and intermediate variable $M(x_l)$ can be obtained by solving the algebraic equations.

Some numerical examples are given to verify the validity of the proposed method in calculating simple boundary conditions and concave boundary conditions as follow.

3. Results and Discussion

Example 1: Figure 3 shows the shallow spherical shell with rectangular bottom on Winkler foundation, and its A-A section is shown in Figure 4. We set $a = b/2 = 100$. The following reference parameters are used: the radius of curvature of the shell $R = 200$, the elastic coefficient of the foundation $k = 200$, thickness of shell $h = 2$, Poisson's ratio $\mu = 0.3$, Young's modulus $E = 2.1 \times 10^6$, the radial load $P_Z = 70$. According to the R-function theory [4], a normalized boundary equation of the first rank can be constructed from the following equation:

$$\omega_0 = \omega_1 + \omega_2 - \sqrt{\omega_1^2 + \omega_2^2} \tag{24}$$

Where $\omega_1 = \frac{a^2 - x_1^2}{2a} \geq 0$, $\omega_2 = \frac{(b - x_2)x_2}{b} \geq 0$.

$\omega_1 = 0$ and $\omega_2 = 0$ denote various parts of the boundary of square shallow spherical shell on Winkler foundation, respectively. The radial deflection curves of line $x_2 = 100$ by the QGFM with four kinds of different square network collocations (as shown in Figure 5) are shown in Figure 6, and the results are compared with those of ANSYS Finite Element Method (FEM). The radial deflection curves of line $x_2 = 0$ for different k and different R by the QGFM with $121(11 \times 11)$ square network and by the ANSYS Finite Element Method (FEM) are shown in Figures 7 and 8 for a comparison, respectively; a good agreement is observed between the two methods.

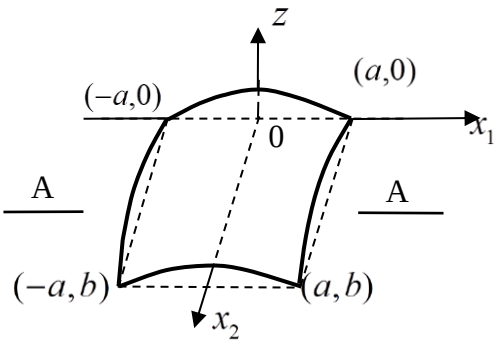

Figure 3. Rectangular shallow spherical shell

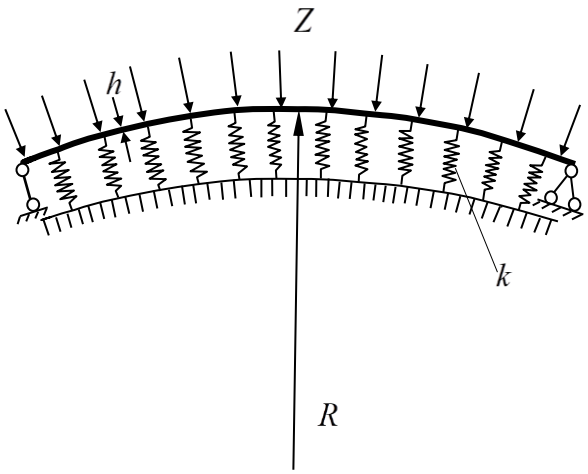

Figure 4. A-A Section

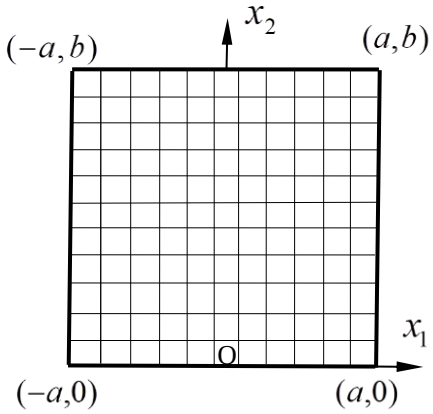

Figure 5. Subdomain division diagram of rectangular integral domain

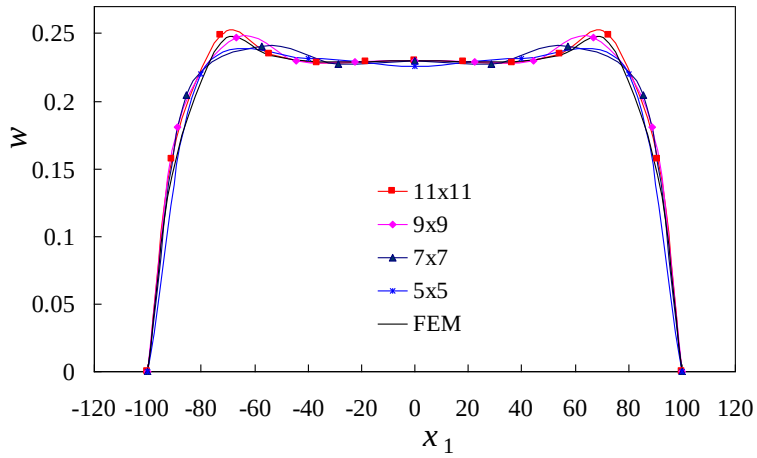

Figure 6. Radial deflection curves of line $x_2 = 100$ in Figure 2 for different square network

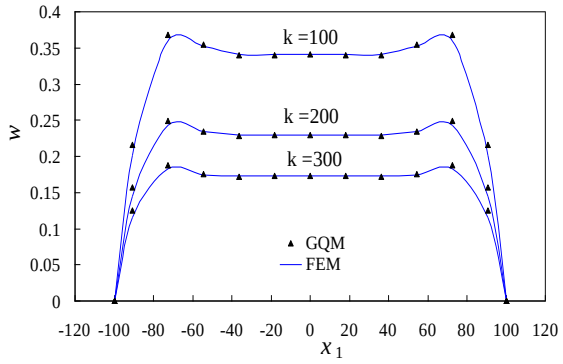

Figure 7. The deflection curve of line $x_2 = 100$ in Figure 2 for different k

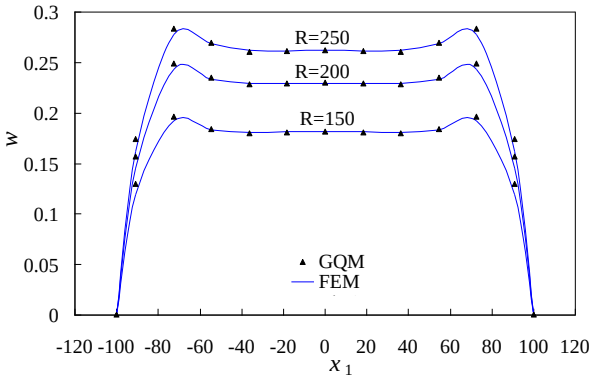

Figure 8. The deflection curve of line $x_2 = 100$ in Figure 2 for different R

Example 2: When we set $a = e = 100, b = d = 60, c = 80$, the shallow spherical shell shown in Figure 3 is a trapezoid shell. The other parameters have the same values as in Example 2. According to the R-function theory [4], a normalized boundary equation of the first rank can be constructed from the following equation:

$$\omega_0 = \omega_1 + \omega_2 + \omega_3 - \sqrt{\omega_1^2 + \omega_2^2} - \sqrt{\omega_1^2 + \omega_3^2} - \sqrt{\omega_2^2 + \omega_3^2} + \sqrt{\omega_1^2 + \omega_2^2 + \omega_3^2} \tag{25}$$

Where $\omega_1 = \frac{(c - x_2)x_2}{c} \geq 0$,

$$\omega_2 = \frac{1}{\sqrt{1 + (\frac{c}{a-b})^2}} (\frac{ac}{a-b} + \frac{c}{a-b} x_1 - x_2) \geq 0$$

$$\omega_3 = \frac{1}{\sqrt{1 + (\frac{c}{e-d})^2}} (\frac{ec}{e-d} - \frac{c}{e-d} x_1 - x_2) \geq 0$$

$\omega_1 = 0, \omega_2 = 0$ and $\omega_3 = 0$ denote various parts of the boundary of trapezoidal shallow spherical shell on Winkler foundation, respectively. The radial deflection curves of line $x_2 = 40$ and $x_1 = 0$ by the QGFM using four kinds of different trapezoidal network collocations (as shown in Figure 8) are shown in Figures 10 and 11, and the results are compared with those of ANSYS Finite Element Method (FEM). The radial deflection curves of line $x_2 = 40$ and $x_1 = 0$ for different k and different R by the QGFM with $121(11 \times 11)$ trapezoidal network and by the ANSYS Finite Element Method (FEM) are shown in Figures 12 to 15 for a comparison, respectively; a good agreement is observed between the two methods.

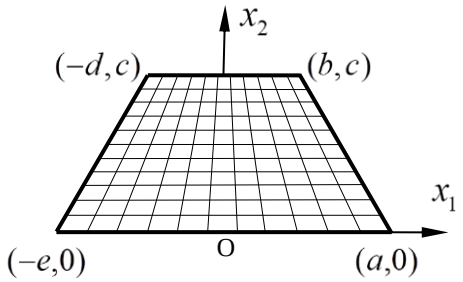

Figure 9. Subdomain division diagram of trapezoidal domain

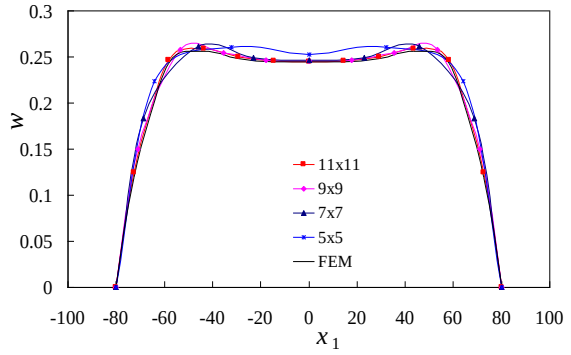

Figure 10. Radial deflection curves of line $x_2 = 40$ in Figure 8 for different trapezoidal network

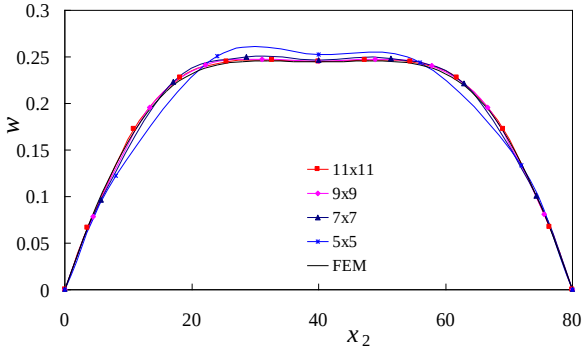

Figure 11. Radial deflection curves of line $x_1 = 0$ in Figure 8 for different trapezoidal network

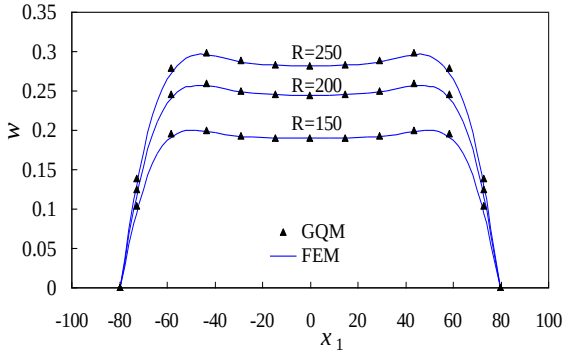

Figure 12. The deflection curve of line $x_2 = 40$ in Figure 8 for different k

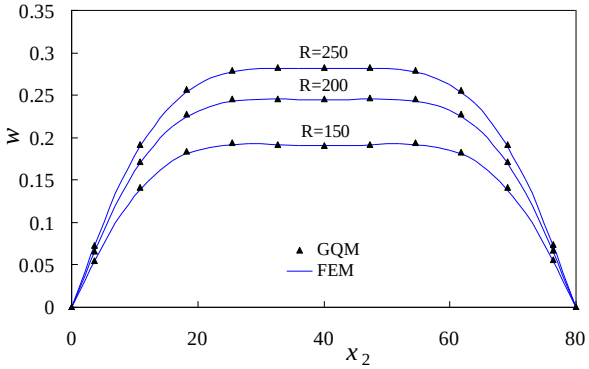

Figure 13. The deflection curve of line $x_1 = 0$ in Figure 8 for different k

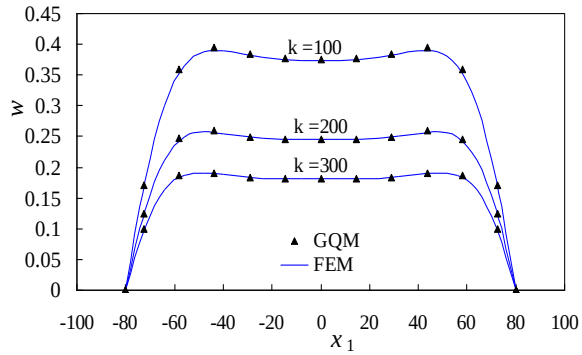

Figure 14. The deflection curve of line $x_2 = 40$ in Figure 8 for different R

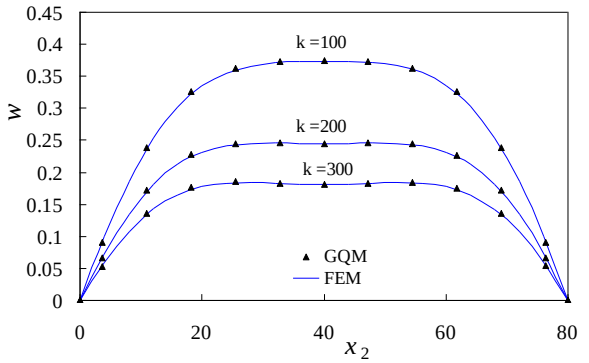

Figure 15. The deflection curve of line $x_1 = 0$ in Figure 8 for different R

Example 3: Figure 16 shows the hexagonal bottom shallow spherical shell on Winkler foundation. We set $a = d = 60$, $b = 100$, $c = 80$, $e = 160$. The other parameters have the same values as in Example 1. According to the R-function theory [4], a normalized boundary equation of the first rank can be constructed from the following equation:

$$\omega_0 = \omega_6 + \omega_7 - \sqrt{\omega_6^2 + \omega_7^2} \tag{26}$$

Where $\omega_6 = \omega_1 + \omega_2 + \omega_3 - \sqrt{\omega_1^2 + \omega_2^2} - \sqrt{\omega_1^2 + \omega_3^2} - \sqrt{\omega_2^2 + \omega_3^2} + \sqrt{\omega_1^2 + \omega_2^2 + \omega_3^2}$,

$$\omega_7 = \omega_4 + \omega_5 - \sqrt{\omega_4^2 + \omega_5^2}$$

In which $\omega_1 = \dfrac{(e - x_2)x_2}{e} \geq 0$

$$\omega_2 = \frac{1}{\sqrt{1 + (\frac{c}{b-a})^2}}(\frac{ac}{b-a} - \frac{c}{b-a}x_1 + x_2) \geq 0, \quad \omega_3 = \frac{1}{\sqrt{1 + (\frac{c}{b-a})^2}}(\frac{ac}{b-a} + \frac{c}{b-a}x_1 + x_2) \geq 0,$$

$$\omega_4 = \frac{1}{\sqrt{1+(\frac{e-c}{d-b})^2}}(c-\frac{e-c}{d-b}b+\frac{e-c}{d-b}x_1-x_2)\geq 0,\quad \omega_5 = \frac{1}{\sqrt{1+(\frac{e-c}{d-b})^2}}(c-\frac{e-c}{d-b}b-\frac{e-c}{d-b}x_1-x_2)\geq 0.$$

$\omega_1 = 0, \omega_2 = 0, \omega_3 = 0, \omega_4 = 0$ and $\omega_5 = 0$ denote various parts of the boundary of hexagonal shallow spherical shell on Winkler foundation, respectively. The radial deflection curves of line $x_2 = c$ and $x_1 = 0$ for different k and different R by the QGFM and by the ANSYS Finite Element Method (FEM) are shown in Figures 17 to 20 for a comparison, respectively; a good agreement is observed between the two methods.

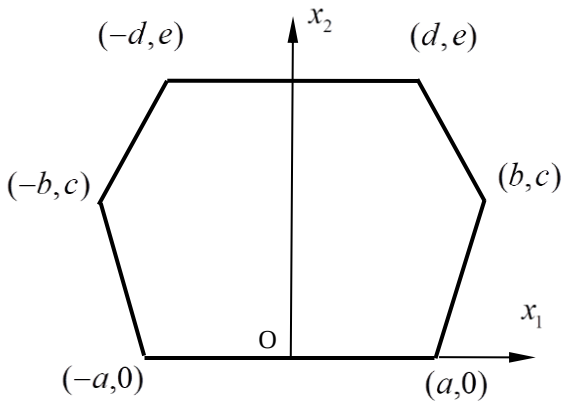

Figure 16. Hexagonal bottom

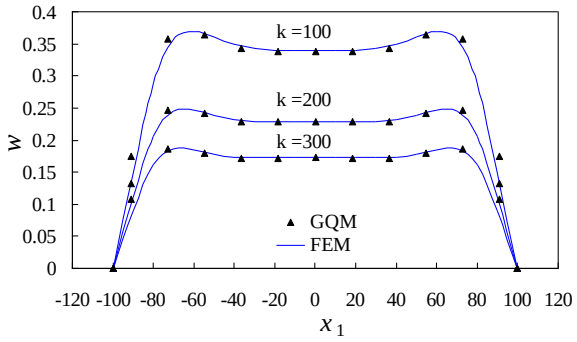

Figure 17. The deflection curve of line $x_2 = c$ in Figure 15 for different k

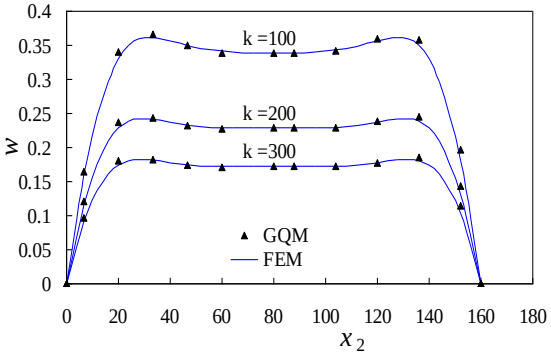

Figure 18. The deflection curve of line $x_1 = 0$ in Figure 15 for different k

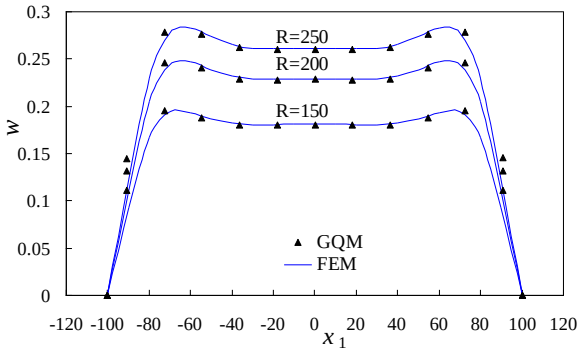

Figure 19. The deflection curve of line $x_2 = c$ in Figure 15 for different R

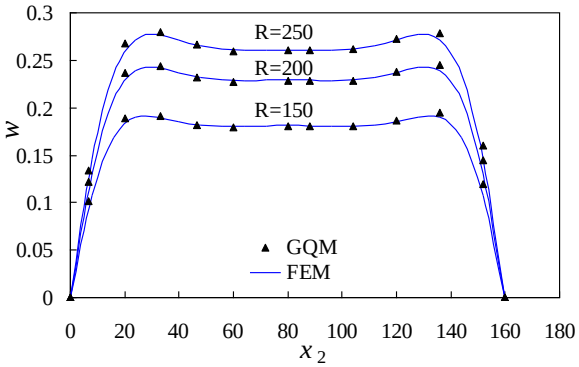

Figure 20. The deflection curve of line $x_1 = 0$ in Figure 15 for different R

4. Conclusion

The radial deflection curves of line $x_2 = 100$ by the QGFM with four kinds of different square network collocations (as shown in Figure 5) are shown in Figure 6, and the results are compared with those of ANSYS Finite Element Method (FEM), which shows the convergence of the present method. The radial deflection curves of line $x_2 = 40$ and $x_1 = 0$ by the QGFM using four kinds of different trapezoidal network collocations (as shown in Figure 8) are shown in Figures 10 and 11, and the results are compared with those of ANSYS Finite Element Method (FEM),

which also shows the convergence of the method. Which shown that the singularity of the kernel of the integral equation and the singular term in the discrete equation are eliminated very good. From the numerical results of the examples, the deflection value decreases with the increase of k and increases with the increase of R. The numerical calculation accuracy is very good, and the results are coincided to the results of FEM nicely.

In the present paper, the R-function theory is used to describe a shallow spherical shell on Winkler foundation with polygonal boundary, and it is applied to construct a quasi-Green's function. The numerical results of the QGFM demonstrate its feasibility, efficiency and rationality by comparing with the FEM solution. The R-function theory can also be applied to effectively solve various boundary value problems of the plates and shells by constructing a trial function that satisfies the complicated boundary shape and by combining with the other method of weighted residuals such as the variational method [22], the spline-approximation [23] and the Ritz method [24].

5. Funding and Acknowledgements

The author would like to express his gratitude especially to his colleagues for helping author preparing this paper. The authors gratefully acknowledge the financial support provided by the Science and Technology Scheme of Guangzhou City (no.201904010141).

6. Conflicts of Interest

The authors declare no conflict of interest.

7. References

[1] Kong, Fan-zhong, Xiao-ping Zheng, and Zhen-han Yao. "Numerical Simulation of 2D Fiber-Reinforced Composites Using Boundary Element Method." Applied Mathematics and Mechanics 26, no. 11 (November 2005): 1515–1522. doi:10.1007/bf03246259..

[2] Šestak, Ivan, and Boško S. Jovanović. "Approximation of Thermoelasticity Contact Problem with Nonmonotone Friction." Applied Mathematics and Mechanics 31, no. 1 (January 2010): 77–86. doi:10.1007/s10483-010-0108-6.

[3] Zhao, Wei-jia, Li-qun Chen, and W. Zu Jean. "A Finite Difference Method for Simulating Transverse Vibrations of an Axially Moving Viscoelastic String." Applied Mathematics and Mechanics 27, no. 1 (January 2006): 23–28. doi:10.1007/s10483-006-0104-1.

[4] Rvachev, V.L. "Theory of R-function and Some of its Application." Kiev: Nauk Dumka (1982):415-421. (in Russian)

[5] Li, Shan-qing, and Hong Yuan. "Quasi-Green's Function Method for Free Vibration of Clamped Thin Plates on Winkler Foundation." Applied Mathematics and Mechanics 32, no. 3 (March 2011): 265–276. doi:10.1007/s10483-011-1412-x.

[6] Yuan, Hong, Shan-qing Li, and Ren-huai Liu. "Green Quasifunction Method for Vibration of Simply-Supported Thin Polygonic Plates on Pasternak Foundation." Applied Mathematics and Mechanics 28, no. 7 (July 2007): 847–853. doi:10.1007/s10483-007-0701-y..

[7] Li, Shanqing, and Hong Yuan. "Green Quasifunction Method for Free Vibration of Clamped Thin Plates." Acta Mechanica Solida Sinica 25, no. 1 (February 2012): 37–45. doi:10.1016/s0894-9166(12)60004-4.

[8] Li, Shan-qing, and Hong Yuan. "Quasi-Green's Function Method for Free Vibration of Simply-Supported Trapezoidal Shallow Spherical Shell." Applied Mathematics and Mechanics 31, no. 5 (May 2010): 635–642. doi:10.1007/s10483-010-0511-7.

[9] Li, Shanqing, and Hong Yuan. "Green Quasifunction Method for Free Vibration of Simply-Supported Trapezoidal Shallow Spherical Shell on Winkler Foundation." Acta Mechanica Solida Sinica 23, no. 4 (August 2010): 370–376. doi:10.1016/s0894-9166(10)60038-9.

[10] Paliwal, D.N., and S.N. Sinha. "Static and Dynamic Behaviour of Shallow Spherical Shells on Winkler Foundation." Thin-Walled Structures 4, no. 6 (January 1986): 411–422. doi:10.1016/0263-8231(86)90038-8.

[11] Majeed, Aaqib, A. Zeeshan, and Shahid Mubbashir. "Vibration Analysis of Carbon Nanotubes Based on Cylindrical Shell by Inducting Winkler and Pasternak Foundations." Mechanics of Advanced Materials and Structures 26, no. 13 (February 5, 2018): 1140–1145. doi:10.1080/15376494.2018.1430282.

[12] Gao, Kang, Wei Gao, Di Wu, and Chongmin Song. "Nonlinear Dynamic Stability of the Orthotropic Functionally Graded Cylindrical Shell Surrounded by Winkler-Pasternak Elastic Foundation Subjected to a Linearly Increasing Load." Journal of Sound and Vibration 415 (February 2018): 147–168. doi:10.1016/j.jsv.2017.11.038.

[13] Banić, Damjan, Michele Bacciocchi, Francesco Tornabene, and Antonio Ferreira. "Influence of Winkler-Pasternak Foundation on the Vibrational Behavior of Plates and Shells Reinforced by Agglomerated Carbon Nanotubes." Applied Sciences 7, no. 12 (November 28, 2017): 1228. doi:10.3390/app7121228.

[14] Wang, Xiancheng, Wei Li, Jianjun Yao, Zhenshuai Wan, Yu Fu, and Tang Sheng. "Free Vibration of Functionally Graded Sandwich Shallow Shells on Winkler and Pasternak Foundations with General Boundary Restraints." Mathematical Problems in Engineering 2019 (March 13, 2019): 1–19. doi:10.1155/2019/7527148.

[15] Shojaeefard, M.H., M. Mahinzare, H. Safarpour, H. Saeidi Googarchin, and M. Ghadiri. "Free Vibration of an Ultra-Fast-Rotating-Induced Cylindrical Nano-Shell Resting on a Winkler Foundation Under Thermo-Electro-Magneto-Elastic Condition." Applied Mathematical Modelling 61 (September 2018): 255–279. doi:10.1016/j.apm.2018.04.015.

[16] Hussain, Muzamal, Muhammad Nawaz Naeem, and Mohammad Reza Isvandzibaei. "Effect of Winkler and Pasternak Elastic Foundation on the Vibration of Rotating Functionally Graded Material Cylindrical Shell." Proceedings of the Institution of Mechanical Engineers, Part C: Journal of Mechanical Engineering Science 232, no. 24 (January 22, 2018): 4564–4577. doi:10.1177/0954406217753459.

[17] Patra, Suchismita, Sudhakar Chaudhary, and V.V.K. Srinivas Kumar. "Approximation of the First Eigenpair of the -Laplace Operator Using WEB-Spline Based Finite Element Method." Engineering Analysis with Boundary Elements 104 (July 2019): 277–287. doi:10.1016/j.enganabound.2019.03.035.

[18] Burman, Erik, Peter Hansbo, Mats G. Larson, Karl Larsson, and André Massing. "Finite Element Approximation of the Laplace–Beltrami Operator on a Surface with Boundary." Numerische Mathematik 141, no. 1 (July 14, 2018): 141–172. doi:10.1007/s00211-018-0990-2.

[19] Prikazchikov, V. G. "Discrete Spectrum of the Laplace Operator for an Arbitrary Triangle with Different Boundary Conditions." Cybernetics and Systems Analysis 55, no. 4 (July 2019): 570–580. doi:10.1007/s10559-019-00166-z.

[20] Mbehou, M. "The Euler-Galerkin Finite Element Method for Nonlocal Diffusion Problems with a p-Laplace-Type Operator." Applicable Analysis 98, no. 11 (February 27, 2018): 2031–2047. doi:10.1080/00036811.2018.1445227.

[21] Ortner, Norbert. "Regularisierte Faltung von Distributionen. Teil 2: Eine Tabelle von Fundamentallösungen." Zeitschrift Für Angewandte Mathematik Und Physik ZAMP 31, no. 1 (January 1980): 155–173. doi:10.1007/bf01601710.

[22] Kurpa, Lidiya, Tatiana Shmatko, and Galina Timchenko. "Free Vibration Analysis of Laminated Shallow Shells with Complex Shape Using the R-Functions Method." Composite Structures 93, no. 1 (December 2010): 225–233. doi:10.1016/j.compstruct.2010.05.016.

[23] Awrejcewicz, J., L. Kurpa, and A. Osetrov. "Investigation of the Stress-Strain State of the Laminated Shallow Shells by R-Functions Method Combined with Spline-Approximation." ZAMM - Journal of Applied Mathematics and Mechanics / Zeitschrift Für Angewandte Mathematik Und Mechanik 91, no. 6 (February 1, 2011): 458–467. doi:10.1002/zamm.201000164.

[24] Kurpa, Lidiya, Tetyana Shmatko, and Jan Awrejcewicz. "Vibration Analysis of Laminated Functionally Graded Shallow Shells with Clamped Cutout of the Complex Form by the Ritz Method and the R-Functions Theory." Latin American Journal of Solids and Structures 16, no. 1 (2019). doi:10.1590/1679-78254911.